Biophys. Struct. Mechanism 1, 169—188 (1975)

X-Ray Small-Angle Studies of the Pyruvate Dehydrogenase Core Complex from *Escherichia coli* K-12

II. Subunit Structure of the Core Complex

Helmut Durchschlag

Institut für Physikalische Chemie der Universität Graz, Austria, and Biochemie II, Universität Regensburg

Received January 7, 1974/Accepted February 23, 1975

Abstract. The interpretation of X-ray small-angle data of the pyruvate dehydrogenase core complex from *E. coli* K-12 reveals the fine structure of the complex. Specific inner surface ($7.07 \cdot 10^{-2}$ Å^{-1}), inner surface ($7.60 \cdot 10^{5}$ Å^{2}), mean transversal length (56.6 Å), coherence length (123.5 Å), structural factor (1.1), and coherence area ($3.27 \cdot 10^{4}$ Å^{2}) have been determined as further structural parameters characterizing the colloidal distribution of matter. Fourier transformations of scattered intensity and of structural amplitude have been carried out and show the existence of slightly disturbed spherical symmetry of the complex built up from subunits. The mean diameter of the three different subunit components of about 78 Å was determined from the correlation function or from the distance distribution. The number of subunits in the complex was ascertained to be 40. The radial excess electron density distribution shows the arrangement of the core complex from a "core" (formed by the transacetylase components) with a small hole inside and a "shell" (formed by the pyruvate dehydrogenase and dihydrolipoamide dehydrogenase components). Although not representing a unique solution, a lot of model calculations indicate how the complex is arranged from subunits. At each edge of a cubic centre, the edge formed by two chains of transacetylase, two chains of pyruvate dehydrogenase and two chains of dihydrolipoamide dehydrogenase components are arranged according to the best fit. Far-reaching conformity between experimental results and model was established.

Key words: Statistic of Intersects — Distance Distribution — Number of Subunits — Radial Electron Density Distribution — Model Calculations.

Introduction

The pyruvate dehydrogenase complex, catalyzing the oxidative decarboxylation of pyruvate, consists of three enzyme components: pyruvate dehydrogenase (enzyme 1, E 1), dihydrolipoamide transacetylase (E 2), and the flavoprotein dihydrolipoamide dehydrogenase (E 3). Binding studies (Koike *et al.*, 1963) confirm that the pyruvate dehydrogenase and the flavoprotein are bound to the transacetylase. When separated from the complex, the pyruvate dehydrogenase and flavoprotein components exist as dimers (Koike *et al.*, 1963; Vogel and Henning 1971). Evidence exists that there are differences in polypeptide chain composition

Enzymes: Pyruvate dehydrogenase complex = pyruvate dehydrogenase (EC 1.2.4.1) plus dihydrolipoamide transacetylase (EC 2.3.1.12) plus dihydrolipoamide dehydrogenase (EC 1.6.4.3).

and some molecular parameters of the *E. coli* K-12 and *E. coli* Crookes complex (*cf.* Dennert and Höglund, 1970; Henning *et al.*, 1972).

On the basis of electron microscope studies of the complex, of subcomplexes and of the enzyme components, models for the arrangement of polypeptide chains in the *E. coli* Crookes enzyme complex have been obtained by Reed and colleagues (Fernández-Morán *et al.*, 1964; Willms *et al.*, 1967; Reed and Oliver, 1968; Eley *et al.*, 1972). Their data indicate that this complex contains 24 pyruvate dehydrogenase, 24 transacetylase and 12 flavoprotein chains. Possible distributions of the pyruvate dehydrogenase and flavoprotein chains around the transacetylase core having cubic shape are discussed by the authors. A modified model for the transacetylase subcomplex was reported by Perham and Thomas (1971).

The pyruvate dehydrogenase complex from *E. coli* K-12 was reported not to be a unique entity in that the amount of the pyruvate dehydrogenase component it contains can vary; however, an enzyme complex with a constant polypeptide chain composition could be isolated (Vogel *et al.*, 1972a, b; Henning *et al.*, 1972). This "core complex" was found to have a molecular weight of $3.8 \cdot 10^6$ and a chain ratio of 16:16:16. These results were confirmed by the author by means of an X-ray small-angle investigation of the core complex in solution (Part I: Overall Structure of the Core Complex; Durchschlag, 1975). The structure of the core complex could be described as a loose assembly of subunits thereby forming a relatively isometric complex of very large extension. Overall structural parameters, like radius of gyration, volume, maximum diameter were investigated. The main aim of this paper is the elucidation of the fine structure of the core complex, which may be derived from the X-ray small-angle data reported in the preceding paper too.

Preliminary reports have been presented (Durchschlag, 1973, 1974).

Experimental Procedure

Preparation of the enzyme, experimental techniques, evaluation procedures *etc.* have been described in detail in Part I.

Results and Discussion

Mainly based on the pioneering theoretical treatment of X-ray small-angle scattering by Porod (1951, 1952, 1967), a lot of further structural parameters may be obtained from the scattering curve of the pyruvate dehydrogenase core complex. For this purpose we will have to define these quantities and check their validity before applying them to biological material in diluted solution. Furthermore it will be shown, that the correlation function not only renders information about dimensions of the particle as a whole but also of subunits. The Fourier transformation of the structural amplitude may be a useful tool for the localization of radial mass distribution also of bodies with slightly disturbed sperical symmetry — provided that there are submaxima in the scattering curve. Hints for the arrangement of subunits in the complex can then be received from model calculations.

Specific Inner Surface, Inner Surface, and Mean Transversal Length

Additional information about the shape of particles can be obtained from the scattering curve by introducing different characteristic numbers which characterize

quite generally the degree of dispersity of colloid systems, namely the mean transversal length and the coherence length. While these numbers have been derived for densely packed systems of unknown structure, they represent also valuable auxiliary means for the characterization especially of multienzyme complexes.

First let us define the specific inner surface as the ratio of the phase-interphase (=inner surface) to the volume of the disperse phase contained in the sample. According to Porod (Porod, 1951, 1952; Kahovec *et al.*, 1953; Kirste and Porod, 1962; Mittelbach and Porod, 1965) the quotient of tail-end constant k_1 and invariant Q (*cf.* Part I) is a direct measure for the inner surface of a two-phase system. The actual relation for the specific inner surface O_S (in Å^2/Å^3) of a system of identical particles is given by

$$O_s = \frac{O}{V_2} = k\, w_1 \cdot \frac{k_1}{Q}, \qquad k = \frac{2\pi^2}{\lambda} = 12.82\ \text{Å}^{-1} \tag{1}$$

$$Q = \int_0^\infty I(2\theta) \cdot (2\theta)^2\, d(2\theta), \qquad w_1 = 1 - w_2 \quad \text{and} \quad w_2 = c_2\, \bar{v}_2,$$

O = inner surface of the particles, V_2 = volume of the particles of the disperse phase (*i.e.* volume V_{exp} obtained from Porod's invariant Q), w_1 = volume fraction of dispersion medium (=of buffer), w_2 = volume fraction of disperse phase (=of protein), and k_1 = tail-end constant.

Concerning the definition of the surface of a macromolecule the same restrictions, of course, are valid as mentioned for the volume (*cf.* Part I).

We obtain for the enzyme core complex a specific inner surface of $O_s = 7.07 \cdot 10^{-2}$ Å^{-1}, and an inner surface of $O = 7.60 \cdot 10^5$ Å^2.

The reciprocal value of the specific inner surface is equivalent with a mean dimension of the particle, the so-called mean transversal length (=intersection length) (Kahovec *et al.*, 1953; Mittelbach and Porod, 1965). This quantity is defined as the mean value of all lengths, which are obtained by intersecting the disperse phase of the system in all directions. For a system of identical particles holds the relation:

$$\bar{l} = \frac{4}{O_s} = \frac{4\, V_2}{O}. \tag{2}$$

The mean transversal length of the enzyme core complex is $\bar{l} = 56.6$ Å.

Coherence Length, Structural Factor, and Coherence Area

The coherence length is in analogy to the mean transversal length or the radius of gyration a measure for the mean largeness of scattering inhomogeneities in a dilute homodisperse system. The coherence length l_c (Porod, 1951, 1952; Kahovec *et al.*, 1953; Mittelbach and Porod, 1965), *i.e.* the double integral width of the correlation function $H(x)$, represents in a two-phase system a measure of the range in which $H(x)$ is different from zero.

$$l_c = 2 \int_0^\infty H(x)\, dx = \frac{\lambda}{2} \cdot \frac{\int_0^\infty I(2\theta) \cdot (2\theta)\, d(2\theta)}{Q}. \tag{3}$$

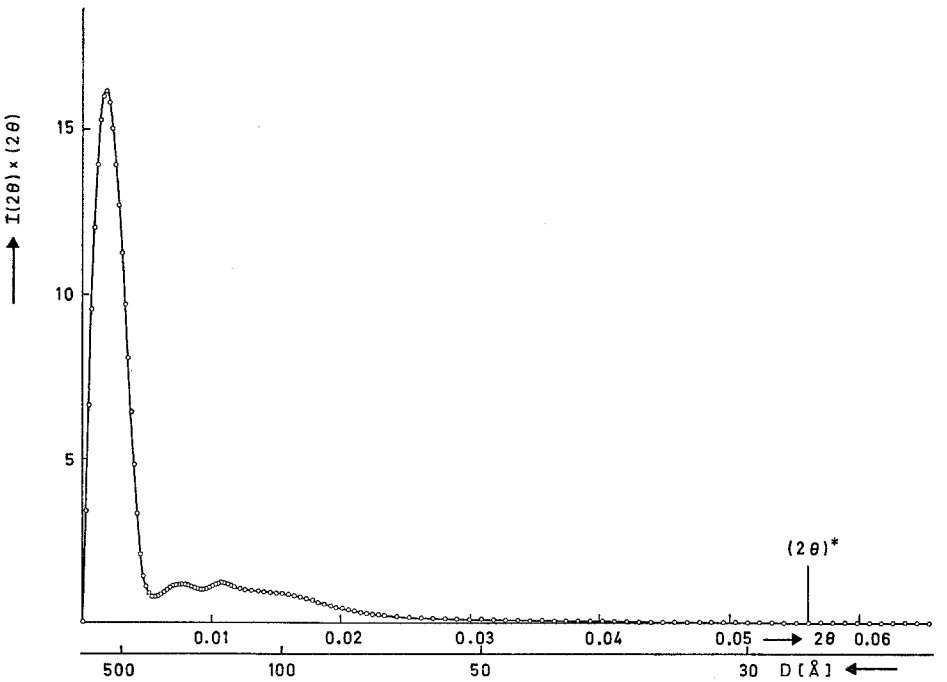

Fig. 1. Plot of $I(2\theta) \cdot (2\theta)$ *vs.* (2θ) for evaluation of the coherence length. $I(2\theta)$ is the intensity of the scattering curve in arbitrary units; (2θ) is the whole scattering angle in rad; D is the Bragg's spacing in Å, calculated from $\lambda = 2\,D \sin\theta$

Fig. 1 shows the plot necessary for evaluation of l_c from $I(2\theta)$ in the above Eq. (3). The coherence length of the enzyme core complex was ascertained to be 123.5 Å as calculated from $I(2\theta)$, this is in good accordance with 123.1 Å as calculated from $H(x)$.

According to a general rule of averaging, the coherence length has always to be larger than the mean transversal length, in general, however, only a bit. In some cases l_c becomes appreciably larger than $\bar{l}$. The term

$$f = l_c/2\,l_r\,, \tag{4}$$

(where $l_r = \bar{l} \cdot w_1 =$ reduced mean transversal length) has been introduced by Kahovec *et al.* (1953) as a number characteristic of the structure. It is a measure for the irregularity of colloidal distribution. For a diluted system of homogeneously filled spherical particles f is about 0.5. Inhomogeneity of electron distribution (*e.g.* with clusters) causes an enlargement of this structural number ($f \approx 1$).

A value for f of 1.10 for the enzyme core complex indicates such an inhomogeneity, a fact which is also explanatory with a loosely packed multienzyme complex composed of subunits. The high value for the inner solvation mentioned in Part I has already pointed into the same direction.

A more vivid explanation for $\bar{l}$, l_c and f of the core complex can be visualized from the following demonstration: A system of single spherical subunits with an

assumed radius of 39 Å ($=\bar{D}_{SU}/2$, *cf.* next paragraph) yields a value for the mean transversal length of 52 Å, whereby for a sphere $\bar{l} = 4/3\,\mathrm{r}$. This number fits quite well with the experimental value of 56.6 Å found for the whole core complex. While the mean transversal length is a purely geometrical property of connected ranges ("inhomogeneity range"), the coherence length depends on the arrangement too. The latter quantity considers all that as a particle which can interfere ("coherence range") whether it is materially connected or not. Thus it is intelligible that the multienzyme complex, which can be regarded as a cluster of spherical subunits, leads to an experimental value for the coherence length of 123.5 Å which is, of course, larger than the value of 58.5 Å obtainable for the single spherical subunits, whereby for a sphere $l_c = 3/2\,\mathrm{r}$. Hence it follows that the factor f is characteristic of the structure of the particle as a whole.

Though no direct meaning can be given to the coherence area a_c (Porod, 1951, 1967; Damaschun and Pürschel, 1968), it may be a useful quantity when comparing the experimental value with that of a model in question.

$$a_c = 2\pi \int_0^\infty H(x) \cdot x\, dx = \frac{\lambda^2}{2\pi} \cdot \frac{\int_0^\infty I(2\theta)\, d(2\theta)}{Q} \cdot \tag{5}$$

The coherence area of the pyruvate dehydrogenase core complex was determined to be $3.27 \cdot 10^4$ Å^2 as calculated from $I(2\theta)$, or $3.25 \cdot 10^4$ Å^2 as calculated from $H(x)$.

Mean Diameter of Subunits

The scattering function of a particle composed of n spherical subunits (Kratky, 1947; Glatter, 1972) can be derived on the basis of the scattering theory of a molecular gas given by Debye (1915, 1930):

$$\Phi(h) = \frac{\sum_{i=1}^{n} \sum_{k=1}^{n} \varphi_i(h,r) \cdot \varphi_k(h,r) \cdot \varrho_i \cdot \varrho_k \cdot V_i \cdot V_k \cdot \frac{\sin h\, d_{ik}}{h\, d_{ik}}}{\sum_{i=1}^{n} \sum_{k=1}^{n} \varrho_i\, \varrho_k\, V_i\, V_k} \tag{6}$$

$$\varphi(h,r) = 3\,\frac{\sin(hr) - (hr)\cos(hr)}{(hr)^3}, \tag{7}$$

where $\Phi(h) = \dfrac{I(h)}{I_0}$ = scattering function, normalized to $\Phi(0) = 1$, $I(h)$ = spherically averaged scattering intensity, I_0 = zero intensity, $h = (4\pi \sin\theta)/\lambda$, $\varphi_i(h,r)$ = normalized scattering amplitude of the ith spherical subunit of radius r, ϱ_i = mean electron density of the ith subunit, V_i = volume of the ith subunit, d_{ik} = distance from the ith to the kth subunit.

The investigation of the long-wave periodicity in the scattering curves at very large angles caused by the arrangement from a large number of subunits permits the elucidation of the substructure of the particle (Glatter, 1972). From the position of the minima in the outer section of the scattering curve the size of identical or very similar subunits can be determined (and not the reciprocal distance of subunits, as one might expect). Recently, this method has been applied successfully for determining the radius of gyration of the subunits of haemocyanin *helix pomatia* (Pilz *et al.*, 1972).

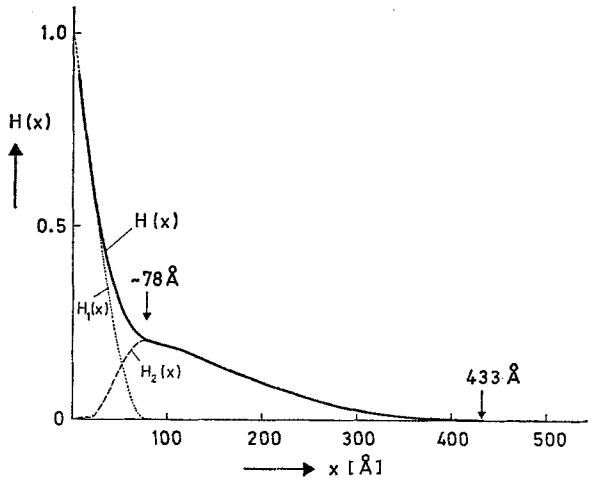

Fig. 2. Correlation function $H(x)$, obtained by a Fourier transformation of the scattered intensity. $H(x)$ delivers the maximum diameter of the particle of 433 Å and the mean diameter of the subunits of 78 Å. $H(x)$ may be separated into two terms $H_1(x)$ and $H_2(x)$ (see text)

The periodicity of the three submaxima of the experimental scattering curve of the pyruvate dehydrogenase core complex (Part I) is caused by the overall structure of the core complex and is a short-wave periodicity, as follows from an examination of the abscissa values of the minima between (the minima of the long-wave periodicity should lie at $h_{o1} = 0.115$ and $h_{o2} = 0.2$ Å^{-1} or so). A nearly total flattening of the minima of the long-wave periodicity is probably due to the different size of the subunits and a slight deviation from the spherical shape of the subunits. Notwithstanding the absence of a distinct long-wave periodicity in the experimental curve an examination of the correlation function $H(x)$ yielded a well defined value for the fine structure of the core complex.

In Part I it was pointed out, that the Fourier transformation of the scattered intensity $I(h)$ yields the correlation function:

$$H(x) = \frac{k}{2\pi^2} \int_0^\infty I(h) \cdot h^2 \frac{\sin hx}{hx} dh \,, \qquad k = \frac{a^2 M}{T_e N P_0 c_2 b \overline{V\varrho^2}} \,, \tag{8}$$

where $= \overline{\varrho^2}$ mean square fluctuation of the electron density (e^2/Å^6). $H(x)$ of a particle that is surrounded by a medium of constant electron density is only different from zero in the interval $0 \leqslant x \leqslant D_{max}$. This property was used to determine the maximum diameter of the particle D_{max} of 433 Å (*cf.* Part I).

A slight break in the curve for the correlation function (Fig. 2) allows the determination of the mean diameter of the subunits $\bar{D}_{SU}$ of the enzyme species present in the complex. About 78 Å are found, whereby from this value alone it cannot be deduced if one subunit is composed of one or two polypeptide chains. It should be stressed that this method of determining the size of subunits can be carried out with the intact complex. No cleavage of the complex by any radical method has to be applied.

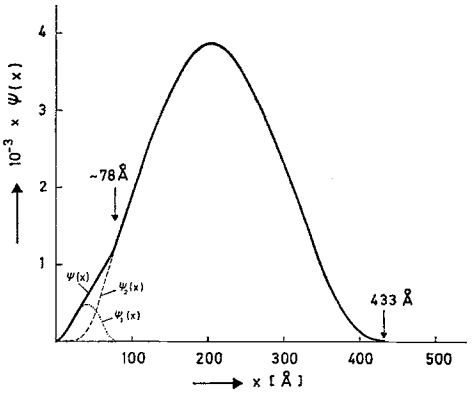

Fig. 3. Distance distribution $\psi(x) = H(x) \cdot x^2$. It is a measure for the frequency of distances x between scattering centres present in the enzyme core complex. $\psi(x)$ may be separated into two terms $\psi_1(x)$ and $\psi_2(x)$ (see text)

The same results concerning diameter of the complex or subunits respectively can be obtained in a more obvious way from the distance distribution. The distance distribution $\psi(x)$ is defined as follows (Kratky and Porod, 1948; Porod, 1948, 1949, 1951): The probability, that the distance between two arbitrarily chosen points of a body lies between x and dx, is given by $\psi(x)\, dx$. $\psi(x)$ corresponds to the correlation function $H(x)$ multiplied by x^2 and is a measure for the frequency of distances x between scattering centres.

As is shown in Fig. 3 the mean diameter of the subunits of the core complex is again emphasized by a break in the distance distribution at an x-value of about 78 Å, indicating that this distance is less frequently present in this complex built up from subunits than in a homogeneous particle. The most frequent distance in the core complex is about 200 Å, but cannot be related to a definite dimension of the molecule. An evident explanation for the maximum diameter of the core complex is given by the fact that there are no distances x in the molecule larger than 433 Å.

Number of Subunits

In order to determine the number of subunits n in the complex, the correlation function $H(x)$ may be separated into two terms $H_1(x)$ and $H_2(x)$:

$H(x)$ and $I(h)$ are given by:

$$H(x) = K_1 \int_0^\infty I(h) \cdot h^2 \cdot \frac{\sin hx}{hx}\, dh \tag{9}$$

$$I(h) = K_2 \sum_{i=1}^{n} \sum_{k=1}^{n} \varrho_i\, V_i\, \varphi_i(h,r)\, \varrho_k\, V_k\, \varphi_k(h,r) \frac{\sin h\, d_{ik}}{h\, d_{ik}} \tag{10}$$

if we split $I(h)$ into two terms

$$I(h) = K_2 \left\{ \sum_{i=1}^{n} (\varrho_i\, V_i)^2\, \varphi_i^2(h,r) + \sum_{i=1}^{n-1} \sum_{k=i+1}^{n} \varrho_i\, V_i\, \varrho_k\, V_k\, \varphi_i(h,r)\, \varphi_k(h,r) \frac{\sin h\, d_{ik}}{h\, d_{ik}} \right\} \tag{11}$$

and insert into Eq. (9), we obtain:

$$H(x) = K_1 K_2 \sum_{i=1}^{n} (\varrho_i V_i)^2 \int_0^\infty \varphi_i^2(h, r) \cdot h^2 \cdot \frac{\sin hx}{hx}\, dh \tag{12}$$

$$+ K_1 K_2 \sum_{i=1}^{n-1} \sum_{k=i+1}^{n} \varrho_i V_i \varrho_k V_k \int_0^\infty \varphi_i(h, r)\, \varphi_k(h, r) \frac{\sin h\, d_{ik}}{h\, d_{ik}} \cdot h^2 \frac{\sin hx}{hx}\, dh$$

$$= H_1(x) + H_2(x) .$$

The first term $H_1(x)$ is given by electron interaction within the subunits. For the case of identical spherical subunits it can be calculated analytically (Porod, 1951):

$$H_1(x) = 1 - \frac{3}{2}\left(\frac{x}{D}\right) + \frac{1}{2}\left(\frac{x}{D}\right)^3 \quad x \leqslant D;\ H(x) = 0,\ x \geqslant D , \tag{13}$$

where D = diameter of the spheres.

The second term $H_2(x)$ represents the interaction of electrons between the subunits, it can be calculated from $H_2(x) = H(x) - H_1(x)$.

For both parts of $H(x)$ one can calculate $\int_0^\infty H(x) \cdot x^2\, dx$ and finds as quotient of both integrals the number of subunits n (Hosemann, 1974)

$$\frac{\int_0^\infty H_1(x) \cdot x^2\, dx}{\int_0^\infty H_2(x) \cdot x^2\, dx} = \frac{n}{n\,(n-1)} . \tag{14}$$

If we apply this method for the pyruvate dehydrogenase core complex using the experimentally found value for $\bar{D}_{SU} = 78$ Å, we obtain for $\int_0^\infty H_1(x) \cdot x^2\, dx = 1.98 \cdot 10^4$ Å^3 and for $\int_0^\infty H_2(x) \cdot x^2\, dx = 8.10 \cdot 10^5$ Å^3. Hence follows $n = 42$ subunits. The separation of $H(x)$ into $H_1(x)$ and $H_2(x)$ and of $H(x) \cdot x^2$ into $H_1(x) \cdot x^2$ and $H_2(x) \cdot x^2$ can also be seen from Figs. 2 and 3.

If we recall the definitions for O, V and $\bar{l}$, further possibilities present for calculating n:

From the quotient of inner surface of the complex ($O = 7.60 \cdot 10^5$ Å^2) and that of one subunit O_{SU} we get n. For spherical subunits holds:

$$n = \frac{O}{O_{SU}}, \qquad O_{SU} = 4\, r^2 \pi , \tag{15}$$

the same holds true for the particle volume ($V = 1.075 \cdot 10^7$ Å^3) and that of one subunit V_{SU}:

$$n = \frac{V}{V_{SU}}, \qquad V_{SU} = \frac{4r^3 \pi}{3} . \tag{16}$$

a) For $r = \frac{3\,\bar{l}}{4} = 42.45$ Å ($\bar{l} = 56.6$ Å), we obtain $O_{SU} = 2.26 \cdot 10^4$ Å^2, hence $n = 34$; and $V_{SU} = 3.20 \cdot 10^5$ Å^3, hence $n = 34$.

b) For $r = \frac{3\,\bar{\bar{l}}}{4} = 40.725$ Å ($\bar{\bar{l}} = 54.3$ Å and $O = 7.91 \cdot 10^5$ Å) we obtain $O_{SU} = 2.08 \cdot 10^4$ Å^2, hence $n = 38$; and $V_{SU} = 2.83 \cdot 10^5$ Å^3, hence $n = 38$.

c) For $r = \frac{\bar{D}_{SU}}{2} = 39$ Å, we obtain $O_{SU} = 1.91 \cdot 10^4$ Å^2, hence $n = 40$; and $V_{SU} = 2.48 \cdot 10^5$ Å^3, hence $n = 43$.

But, the calculation of n from the experimental $\bar{l}$ (example *a*) must give a bit too low value for n, because $\bar{l}$ of a complex consisting of touching subunits cannot be completely identical with $\bar{l}$ of single subunits. This can easily be shown by using $\bar{\bar{l}}$ and O from Table 1 (example b). Therefore, a more reliable result will be found by calculating n from $\bar{D}_{SU}$ (example c).

Summing up, $n \approx 40$ will be an obvious approach for the number of subunits. Remaining slight deviations obtained with the different methods may be due to deviations from the spherical shape of the subunits and to the fact that the electron density within one subunit is not a constant.

An additional but more ambiguous method for determining n comes from the comparison of the experimental scattering curve with theoretical ones built up from different mass centres (*i.e.* subunits). As will be shown independently of the above mentioned methods, this again yields 40 subunits (*cf.* section on Model Calculations).

Radial Excess Electron Density Distribution

With bodies showing spherical symmetry the structural amplitude (*i.e.* the square root of the scattering intensity) becomes independent of the position of the particle relative to the X-ray beam. In this case the scattering intensity includes not only the statistic of distances, but additionally the information about the arrangement of scattering centres within the particles, that is to say the radial packing density of scattering centres. By means of a Fourier transformation of the structural amplitude $F(h)$ the radial excess electron density distribution $\varrho(r)$ can be obtained (Anderegg *et al.*, 1961, 1963; Fischbach *et al.*, 1965; Harrison, 1969; Zipper *et al.*, 1971, 1973).

$$\varrho(r) = \frac{k}{2\pi^2} \int_0^\infty F(h) \cdot h^2 \frac{\sin hr}{hr}\, dh\,, \qquad k = \sqrt{\frac{a^2 M}{T_e \bar{N} P_0 c_2 b}}\,. \tag{17}$$

$\varrho(r)$ (in e/Å^3) represents the spherically averaged difference of electron density of particle and solvent at a distance r from the particle centre. The more submaxima can be measured in a scattering curve with sufficient accuracy, the higher is the accuracy of the electron density distribution obtained. This, of course, holds only for submaxima caused by the overall structure of the particle. (The substructure, which is responsible for the long-wave periodicity, may also lead to a disturbance of these submaxima.)

But before applying this procedure, one has to establish the existence of spherical symmetry. It can be proved by the fact that the main maximum and submaxima of the scattering curve as well as submaxima among themselves are separated by minima going to zero positions, where the scattering intensity actually decreases to the value zero. Deviations from spherical symmetry cause deviations from this ideal course of the scattering curve, mainly due to anisometry of the particle and/or inhomogeneity within the particle (*e.g.* arrangement from subunits). Disturbances of spherical symmetry cause the electron density distribution to be replaced by an alternative function. Of course, the more the particle

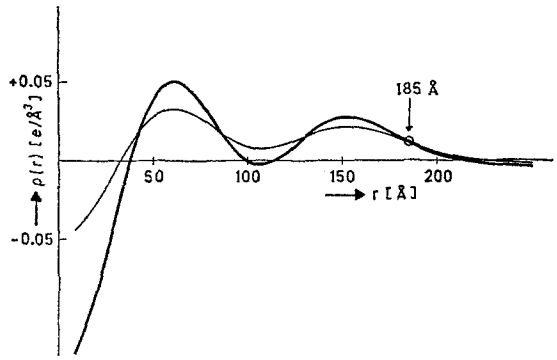

Fig. 4. Apparent radial distribution of excess electron density $\varrho(r)$ of the enzyme core complex, obtained by a Fourier transformation of the structural amplitude. Full line, function without any artificial temperature factor; thin line, function with an artificial temperature factor. $\varrho(r)$ indicates two accumulations of mass: a core (formed by the transacetylase components) and a shell (formed by pyruvate dehydrogenase and flavoprotein components). The negative values of $\varrho(r)$ at small r-values are caused by termination effects of the Fourier transformation, they rather indicate a small hole inside the core. The radius of a substitute sphere can be determined from the intersections of the curves at 185 Å

deviates from the spherical form, the less is the accordance between particle and substitute sphere. The quotient of experimentally determined radius of gyration and the radius of gyration of a substitute sphere, or of the maximum diameter and mean diameter of this substitute sphere, can be used as a measure for this deviation.

As could be seen from Figs. 1 or 6 of Part I the scattering curve of the enzyme core complex indicates a remarkable deviation from the ideal course of a mere sphere or a body with spherical symmetry by showing that the intensity minima do not reach the abscissa. The problem how to obtain an amplitude curve with alternating signs was therefore resolved according to Fischbach *et al.* (1965) by using the intensity maxima to locate the maxima and minima of the amplitude curve and connecting these with a smooth curve crossing the abscissa (*cf.* Zipper *et al.*, 1971).

In consequence of the ill-conditioned minima and the existence of only three submaxima in the experimental scattering curve we will not draw too sophisticated conclusions from the radial excess electron density distribution. A strong termination effect may give rise to falsifications of the result. In such a case only in connection with model calculations, and only then, an interpretation gives indications of an actual mass distribution. So will confine ourselves to some statements:

The radial excess electron density distribution (Fig. 4) does not show a uniform course. The appearance of two maxima may be explained by two radial accumulations of mass in the core complex: a "core" of high excess electron density and a broad "shell" of lower excess electron density. As will be discussed later on, the inner accumulation of mass is due to the transacetylase components, which form the cubic centre of the core complex, the second is due to the pyruvate

dehydrogenase and flavoprotein components, which encircle the inner core of the complex thus forming the broad, but less dense shell of the complex. This lower density of the shell may be interpreted by the variation of size and arrangement of these two different subunit species. The variation of the thickness of the shell and especially the fact that there is no large hollow space (with different electron density) between inner and outer range confirms the absence of a thickness factor (*cf.* Part I) of the "shell" of the core complex.

The strong decrease of $\varrho(r)$ at small r-values (that means near the central point of the core complex) is caused by the abrupt cut-off of the amplitude curve. This termination effect can be modified by introduction of a Gaussian artificial temperature factor as is shown in Fig. 4. The decrease of $\varrho(r)$ at small r-values rather indicates a small hole inside the transacetylase core [where $\varrho(r)$ should be zero] than negative values of $\varrho(r)$.

It should be noted that the existence and the course of the two maxima in the electron density distribution as well as the hole inside the core are not mere artifacts due to the calculation from only 3 submaxima of the experimental scattering curve (corresponding to a resolution of $\Delta = \pi/h_\omega = 35.7$ Å). By means of Fourier transformations of the theoretical scattering curve of the model discussed later on it could be proved that their resulted a nearly identical behaviour of the electron density distribution when cutting off the amplitude curve after the 3rd, 4th or 5th submaximum (corresponding to differently high resolutions).

The radial excess electron density distribution of the enzyme core complex allows the determination of a mean radius of a substitute sphere of the type described before. The intersection of the curves at 185 Å (Fig. 4) may be considered as mean radius of such a substitute sphere. It is quite reasonable that the maximum diameter of the enzyme core complex of 433 Å, obtained from the correlation function by a Fourier transformation of the scattering intensity, is larger than the mean diameter of the substitute sphere of 370 Å, obtained from the radial excess electron density distribution by means of a Fourier transformation of the structural amplitude.

This mean value for the diameter of the substitute sphere is at the same time the minimum diameter the particle could have at all, assuming ideal spherical symmetry. Because there is only perturbed spherical symmetry the actual diameter of the particle must be larger than this value (namely 433 Å). On the other hand, the not too large discrepancy between the two values shows a not too large deviation from spherical symmetry of the overall complex. In connection with the comparison of experimental and theoretical scattering curves (Part I and next paragraph) it indicates the arrangement of the complex from subunits rather than anisometry.

A comparison of the corresponding values for the radii of gyration leads, of course, to the same result: $R_{exp} = 156.5$ Å must be larger than R of the substitute sphere of 143.3 Å in consequence of perturbed spherical symmetry. Furthermore a purely hypothetical radius of gyration can be obtained under assumption of a homogeneous sphere using the experimentally ascertained volume of the particle or the dry volume: R (from V_{exp}) = 106.0 Å, R (from V_{calc}) = 78.6 Å. The latter contradictions to the experimentally found value of R can easily be removed by the assumption of hollow spaces within the multienzyme complex composed of

subunits. These cavities cause the enlargement of the radius of gyration as a result of the position of scattering centres arranged now more loosely and thus more distant from the centre of gravity of electrons. Or to say it in other words, the experimentally found high value of $R_{exp} = 156.5$ Å unequivocally establishes the loose structure of the core complex and excludes a simple solid body as a model for the complex.

Model Calculations

A comparison of the experimental scattering curve with theoretical ones, calculated for simple full or hollow bodies, showed the overall structure of the core complex to be relatively isometric (Part I). But, the comparison did not bring about satisfactory agreement in the range of the submaxima, probably due to the arrangement of the complex from subunits. The calculation of theoretical scattering curves of bodies built up from subunits of different shape and arrangement could possibly lead to a further refinement (*cf.* Durchschlag *et al.*, 1971). In order to use this pure trial and error method as a tool for more detailed model calculations, it is appropriate to make use of the information concerning complex and subunits obtained so far from this investigation and the investigations of others.

For the following model calculations let us take for granted the following results and assumptions:

1. molecular weight of the enzyme core complex (Part I);
2. volume of the enzyme core complex (Part I);
3. molecular weights of the polypeptide chains of the enzyme components (Vogel *et al.*, 1971; Vogel and Henning, 1971, 1973; *cf.* Part I);
4. ratio of polypeptide chains of enzyme components of 16:16:16 (*cf.* Part I);
5. assumption of spherical subunits representing one or two polypeptide chains of the enzyme components;
6. assumption, that the centre of the complex is somehow formed by transacetylase subunits surrounded somehow by pyruvate dehydrogenase and flavoprotein components in analogy to the *E. coli* Crookes enzyme complex (Reed and Oliver, 1968) and the own findings of the radial excess electron density distribution. No further information concerning arrangement of subunits within the *E. coli* K-12 complex was obtainable.

Following this line, about 150 calculations of theoretical scattering curves according to Eqs. (6) and (7) were carried out, whereby the number of scattering centres and especially their coordinates (*i.e.* the position of the subunits to each other) were varied. The number of scattering centres is given from the question whether the monomer or dimer formation of enzyme components is approximated by a sphere. But, of course, "monomer" does not necessarily mean that it really exists as a monomer in the complex. This conclusion can only be drawn from small-angle experiments, when the monomers are spatially separated.

In the following, models built up from 24, 32, 40 and 48 centres were computed, at the same time varying the arrangement of subunits. The radii of these spherical subunits are given in Table 1. The best fits were varied furthermore by slight changes of coordinates until a most optimal accordance between experimental and theoretical scattering curve was gained. The essential criterion for the validity of a definite body equivalent in scattering is the right course of the scattering

Table 1. Comparison of the values for mean diameter $\bar{D}_{SU}$ of the subunits, for mean transversal length $\bar{l}$, and for the inner surface O of the core complex obtained from models and experimental scattering curve respectively. The model bodies are built up from n spheres of radius r, each sphere representing one subunit composed of one or two polypeptide chains. The ratio γ of subunits of the enzyme components E 1, E 2 and E 3 in the core complex varies depending on the assumed model. A ratio of chains of 16:16:16 is assumed for all models

	n	γ (E 1:E 2:E 3)	r_{E1} (Å)	r_{E2} (Å)	r_{E3} (Å)	$\bar{D}_{SU}$ (Å)	$\bar{\bar{l}}$ (Å)	O (Å^2)
model	24	8:8:8	51.4	47.7	42.4	94.3	63.6[a]	$6.75 \cdot 10^{5}$[b]
	32	8:8:16	51.4	47.7	33.6	83.2	59.5[a]	$7.22 \cdot 10^{5}$[b]
	40	16:8:16	40.8	47.7	33.6	78.6[c]	54.3[a, c]	$7.91 \cdot 10^{5}$[b, c]
	48	16:16:16	40.8	37.9	33.6	74.9	50.5[a]	$8.50 \cdot 10^{5}$[b]
experiment						78	56.6	$7.60 \cdot 10^{5}$

[a] Calculated for a mixture of subunits according to $\bar{\bar{l}} = \sum_{i=1}^{3} n_i p_i^2 \bar{l}_i / (\sum_{i=1}^{3} n_i p_i^2)$ (Mittelbach and Porod, 1965), where p_i = factor due to a linear extension of subunit species i, n_i = number of subunit species i, $\bar{l}_i$ = mean transversal length of subunit species i.

[b] Calculated from the sum of surfaces of all subunits.

[c] From the best fit of theoretical scattering curves of 40 mass centres (*cf.* Table 2) we obtain $\bar{D}_{SU} = 78$ Å, $\bar{l} = 55.6$ Å, and $O = 7.59 \cdot 10^5$ Å^2; there is excellent agreement between these values and those from the experiment.

curve in the angular range of the main maximum as well as submaxima. Moreover, the model has to yield at least similar values for the parameters obtainable from the scattering curve and its Fourier transformed function. As a first check the values for radius of gyration and maximum diameter may be used.

For simple reasons we will only summarize the most important conclusions resulting from these model calculations. No appropriate fit was found with models from 24 centres (all spheres representing dimers) or 48 centres (all spheres representing monomers), though these models might be the most obvious ones. For example, all the scattering curves from models of 24 centres showed in the range of the first submaximum a higher intensity than the experimental curve, obviously because the inner cavities of a body built up from 24 spheres in any optional arrangement are too large. Similarly, no good fit was obtained for models built up from 32 subunits.

As can be seen from Table 1, a comparison of the values for mean diameter of the subunits, for mean transversal length, and for the inner surface of the complex of the diverse models on the one hand and the experimental results on the other substantiate these findings. Only in the case of the models from 40 centres there exists agreement. It is quite logical, that the experimentally determined value for the inner surface of the core complex is slightly smaller than the value obtained from the sum of surfaces of all subunits of the model, because touching subunits cause a smaller total surface. The same reason is responsible for the small discrepancies in the values for $\bar{l}$.

Fig. 5 depicts the comparison of the experimental curve and of the best fit of theoretical scattering curves of models from 40 centres and at the same time this

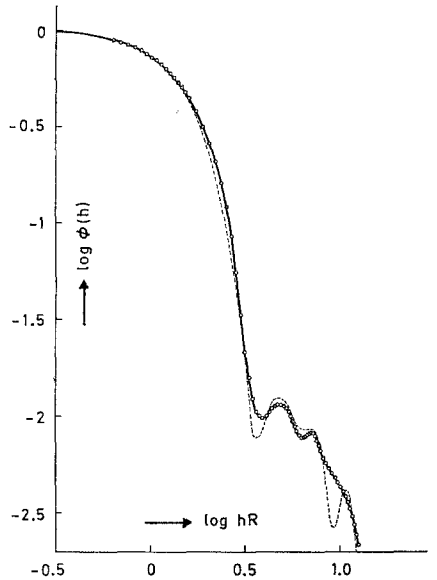

Fig. 5. Log-log plot for comparison of the experimental scattering curve (o) of the enzyme core complex with the best fit of theoretical scattering curves of model complexes built up from subunits. The model is shown in Fig. 6. Good agreement between experimental and theoretical scattering curves was obtained

is the best fit of all (E2 dimer spheres, E1 and E3 touching monomer spheres). In the range of the main maximum as well as the first and second submaximum there is good agreement in respect to position and height, only in the range of the third submaximum a rough agreement exists. The lack of accordance in the range of the minima is probably due to a lack in spherical symmetry. Moreover, because model bodies presuppose some idealizations, slight deviations from the ideal course, especially in the range of higher submaxima, are not very surprising. On the other hand, I am sure, by an immense number of further model calculations a slightly improved agreement could be obtained. But considering the assumptions previously mentioned, such a model would not represent more reality than the model given below.

The model shown in Fig. 6 and representing the best fit is characterized by the following features: The centre of the core complex from *E. coli* K-12 is formed by the transacetylase subunits, each subunit representing two polypeptide chains. These subunits are arranged in form of a cube producing at the same time a small cavity inside the cube. Some other arrangements for the transacetylase subcomplex turned out to be incompatible with the model calculations when compared with the experimental scattering curve. The pyruvate dehydrogenase and flavoprotein subunits are arranged around the transacetylase subcomplex as shown in the figure. Larger cavities are not present in the molecule, but all subunits form a loose packing thus constituting a lot of smaller cavities between.

The proposed model also takes into account the biochemical function in so far as there is contact guaranteed between transacetylase and pyruvate dehydrogenase

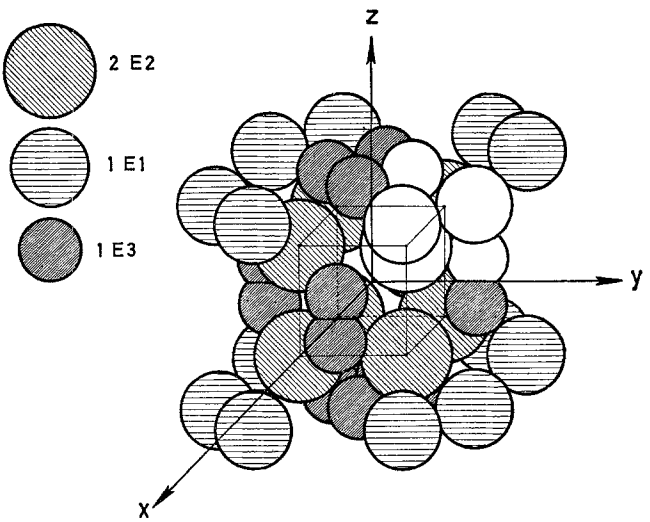

Fig. 6. Model for the enzyme core complex consisting of 40 mass centres. The spheres represent two polypeptide chains of the transacetylase (E2) component or one chain of the pyruvate dehydrogenase (E1) or flavoprotein (E3) component. The centre of the complex is formed by cubic arrangement of E2 subunits, which are surrounded by E1 and E3 subunits. The subunits belonging to an edge of the cube (thus forming the smallest geometrical unit) are illustrated by a lack of hatching

or transacetylase and flavoprotein components respectively. The transfer of reaction products to the other two enzymes as well as to CoA is possible by means of the flexible arm of the transacetylase component (*cf.* Reed and Oliver, 1968).

The cubic arrangement for the transacetylase components is an analogy to the results obtained by Reed and Oliver (1968) for the *E. coli* Crookes enzyme complex, though these authors presuppose one subunit to be composed of three chains. The electron micrographs obtained by Reed and Oliver showed that a subcomplex consisting of pyruvate dehydrogenase and transacetylase subunits delivers nearly the same picture as a graph obtained from the whole complex, suggesting that the flavoprotein molecules are obscured by pyruvate dehydrogenase molecules. The X-ray small-angle scattering corroborates this finding also for the *E. coli* K-12 complex by the fact that the maximum diameter of the core complex is formed by the pyruvate dehydrogenase subunits. The pyruvate dehydrogenase particles form the peripheral units of the core complex. The enclosure of the flavoprotein subunits in the complex does not change the overall picture of the complex very drastically.

The large extension of the core complex from *E. coli* K-12 was proven conclusively and independently of any preconceived model by the determination that the radius of gyration was 156.5 Å and the maximum diameter of the particle 433 Å (Part I). The fact, that already the core complex from *E. coli* K-12 is considerably larger (the complex, from which excess pyruvate dehydrogenase has not been removed, might be still a bit larger) than the complex from *E. coli* Crookes, for which a maximum diameter of 300 Å has been reported

several times by Reed and collaborators (Fernández-Morán *et al.*, 1964; Willms *et al.*, 1967; Reed and Oliver, 1968), additionally confirms their different molecular design.

Based on the model shown above, the absolute dimensions of the model can now be calculated: diameter of the hole inside the transacetylase cube: 103 Å; side-length of the transacetylase cube: 210 Å; its maximum diameter: 294 Å; maximum diameter of the core complex: 463 Å (these "maximum diameters" have been calculated between the two utmost points of the corresponding subunit spheres of the model; *cf.* remarks in Part I). A quantitative interpretation of the radial excess electron density distribution in terms of these dimensions is not possible because of the formerly mentioned restrictions.

Slight overlapping of the spheres of the model (like the flavoprotein spheres in Fig. 6) or small spaces between them are insignificant and do not implicitely reflect physical reality, their existence gives indications that deformed spheres would rather fit the experimental data than the assumption of mere spherical subunits. The more essential parameter for the calculation of theoretical scattering curves is the position of the scattering centres represented by the centres of the spheres.

Though the mentioned space-filling model reflects only an idealized shape, a body equivalent in scattering, the actual distribution of mass in the core complex will not be very far from the given model, because otherwise there would be no accordance in the course of theoretical and experimental scattering curves to such an extent as shown before. As has been pointed out, slight deviations of subunit coordinates already cause an essential different course of the scattering curve. The height and position of submaxima is caused, as has been shown by the model calculations carried out so far, not only by the volume of cavities, as with hollow spheres or hollow cylinders for example, but also by the mutual arrangement of subunits. *Vice versa*, from a given course of the experimental scattering curve an approximate position of mass centres (*i.e.* of subunits) can be deduced.

Moreover, a crucial criterion for the accordance of proposed model and experimental result is — in addition to the comparison of scattering curves — the critical comparison of diverse molecular parameters obtained from small-angle scattering. As can be seen from Table 2, the accordance was excellent. At the same time this accordance of scattering curves and parameters obtained from them verifies the assumption of a model of 40 spherical subunits of the size proposed and proves the ratio of polypeptide chains of the three different enzyme components in the core complex of 16:16:16 to be correct.

Furthermore, the data obtained from $I(2\theta)$ or $H(x)$ respectively show excellent agreement (*e.g.* the values for l_c, a_c, v_c in Table 2). Hence follows, that the objections against practical use of the Fourier transformation because of lacking accuracy (Porod, 1967) have lost their validity. This is probably due to the higher accuracy of scattering measurements nowadays.

From small-angle experiments alone, no correlation between structure and function of subunits and complex can be given. According to the model given above, there is (in the absence of substrates and cofactors) an asymmetric distribution of the flavoprotein subunits in the complex: On each edge of the cube two polypeptide chains of transacetylase (forming a dimer subunit) are situated,

Table 2. Comparison of the values for diverse molecular parameters obtained from experimental scattering curve, theoretical scattering curve of the model, and model itself

property	calculated from	experimental curve	theoretical curve	model
M_r	I_0, P_0	$3.78 \cdot 10^6$[a]		$3.776 \cdot 10^6$
R (Å)	$I(2\theta)$, according to Guinier	165	154—162[b]	151.8[c]
R (Å)	$H(x)$	156.5	151.6[d]	
l_c (Å)	$I(2\theta)$	123.5	131.7[e]	
l_c (Å)	$H(x)$	123.1	131.6[d, e]	
a_c (Å^2)	$I(2\theta)$	$3.27 \cdot 10^4$	$3.40 \cdot 10^4$[e]	
a_c (Å^2)	$H(x)$	$3.25 \cdot 10^4$	$3.41 \cdot 10^4$[d, e]	
v_c (Å^3)	$I(2\theta)$	$1.075 \cdot 10^7$[a]	$1.06 \cdot 10^7$	$1.074 \cdot 10^7$
v_c (Å^3)	$H(x)$	$1.04 \cdot 10^7$	$1.06 \cdot 10^7$[d]	
O_s (Å^{-1})	$I(2\theta)$	$7.07 \cdot 10^{-2}$	$7.20 \cdot 10^{-2}$	
O (Å^2)	$I(2\theta)$	$7.60 \cdot 10^5$	$7.59 \cdot 10^5$	$7.91 \cdot 10^5$[f]
$\bar{l}$ (Å)	$I(2\theta)$	56.6	55.6[e]	54.3[g]
f	$I(2\theta)$	1.10	1.19[e]	
D_{max} (Å)	$H(x)$	433[h]	439[d]	463[i]
D_{SU} (Å)	$H(x)$	78	78[d]	78.6
n	$H(x)$	42	43[d]	40
n	D_{SU}, O	40	40	
n	D_{SU}, v_c	43	43	
n	$\bar{l}$, O	34	35	
n	$\bar{l}$, v_c	34	35	

[a] These quantities have been used for calculating the model.

[b] The result depends on the angular range used for determination of the slope of the Guinier straight line.

[c] Calculated from the coordinates of the subunits of the model.

[d] Whereby the theoretical scattering curve for the Fourier transformation was terminated at the same angle $h = 0.39$ Å^{-1} as the experimental scattering curve.

[e] Indicates slight idealizations of the model rather than a deviation.

[f] Calculated from the sum of surfaces of all subunits.

[g] Calculated for a mixture of subunits, for details see annotation [a] in Table 1.

[h] Distance between the two utmost points of the core complex will be about 457 Å (in analogy to the values from model and theoretical curve).

[i] Distance between the two utmost points of the particle (*cf.* Part I).

which are surrounded by two chains of pyruvate dehydrogenase (probably forming a dimer) and two chains of the flavoprotein (possibly each chain of them forming a dimer with a chain of another edge). Explanations for this behaviour may be the possibility of sticking together of all subunits to the whole complex for energetic reasons, thus showing the necessity to form a so large complex, such a superstructure which is larger than the geometrical unit composed only of one pyruvate dehydrogenase, one transacetylase and one flavoprotein dimer subunit. On the other hand, a complete complex is not necessary for enzymatic catalysis (Schwartz and Reed, 1969; Henning *et al.*, 1972). The smallest functional subunit was reported to have a molecular weight of about $5 \cdot 10^5$ (Schwartz and Reed, 1969), which is about one eighth the value of the core complex. But explanations for this behaviour must always be ambiguous when considered only from the

physico-chemical point of view. To what extent evolutionary chance events are concerned with this problems or not, cannot be answered unequivocally at the present state (*cf.* Vogel *et al.*, 1972b).

According to the model proposed above there might result a different binding behaviour of the flavoprotein chains. Another question, but closely connected with this problem, is how the "excess" six pyruvate dehydrogenase chains can be bound to the core complex. The fact that they can easily be removed during the preparation procudure shows that they are bound differently (Vogel *et al.*, 1972a, b). A simple answer to this question might be, that they are bound at the six sides of the cube to the flavoprotein components [which could also include the possibility of aggregation or of further binding (to the membrane ?) by means of these monomer chains]. Further binding studies and X-ray investigations of the 1.35:1:1 complex should be able to clear up where these "excess" pyruvate dehydrogenase chains are bound [*e.g.* by determination of D_{max} or $\varrho(r)$].

Summarizing we may state the puzzling fact, that in spite of some striking similarities between the two pyruvate dehydrogenase complexes from *E. coli* K-12 and Crookes strain there remain a lot of differences between them. As has been pointed out, the similarities are restricted to the rough structural design (*e.g.* cubic arrangement of the transacetylase subcomplex, peripheral subunits in the complex are the pyruvate dehydrogenase chains), while, according to the data obtained so far, the fine structure of the complexes seems to be very different (*e.g.* different polypeptide chain ratio, different size of complex, of transacetylase subcomplex and of peripheral subunits, different electrophoretic and hydrodynamic behaviour). An obvious corollary of these different data is the dissimilarity of the models proposed for the complexes. A direct comparison of the models in terms of scattering curves is not possible until enough numerical material will be gained by an X-ray examination of the *E. coli* K-12 complex, from which excess pyruvate dehydrogenase has not been removed (1.35:1:1 complex) as well as of the *E. coli* Crookes complex. It is to be hoped that further X-ray investigations like this will throw some light upon these problems in order to obtain additional evidence for a tentative model and to gain further insight into the macromolecular organization of these multienzyme complexes.

While the experimental technique of X-ray small-angle scattering has been used successfully for the investigation of a lot of other enzymes, the results reported in this paper represent the first demonstration of its application of parameters like diameter of subunits obtained from the correlation function, statistic of intersects and structural factor to biological samples, whereby multienzyme complexes can be considered as ideal examples of their usefulness. The findings also show for the first time the possibility to determine the number of subunits and to localize possible arrangements of subunits in a multienzyme complex by means of this method. The investigation of multienzyme complexes can be regarded as one of the most outstanding challenges to small-angle scattering.

Acknowledgements. The author expresses gratitude to Professor Dr. Dr. h.c. Otto Kratky, in whose laboratory in Graz the work was carried out, for his kind interest in the problem. The author is much indebted to Dr. Peter Zipper, Graz, for helpful and stimulating discussions. Part of the evaluation work was done during a stay in Professor Dr. Rainer Jaenicke's biochemical group in Regensburg. This stay was made possible by an EMBO long-term

fellowship awarded to the author. Sincerest thanks are also due to Professor Dr. Ulf Henning and Dr. Otto Vogel from the Max-Planck-Institut für Biologie, Tübingen, for the generous gift of the enzyme.

Calculations were performed on a UNIVAC 494 computer in the Rechenzentrum Graz and on a SIEMENS 4004/45-G computer in the Rechenzentrum Universität Regensburg.

References

Anderegg, J. W., Geil, P. H., Beeman, W. W., Kaesberg, P.: An X-ray scattering investigation of wild cucumber mosaic virus and a related protein. Biophys. J. **1**, 657—667 (1961)

Anderegg, J. W., Wright, M., Kaesberg, P.: An X-ray scattering study of bromegrass mosaic virus. Biophys. J. **3**, 175—182 (1963)

Damaschun, G., Pürschel, H.-V.: Die Ermittlung der Abmessungen gelöster Makromoleküle aus Röntgen-Kleinwinkeldiagrammen mittels der Charakteristikflächen. Acta biol. med. germ. **21**, 567—569 (1968)

Debye, P.: Zerstreuung von Röntgenstrahlen. Ann. Physik **46**, 809—823 (1915)

Debye, P.: Röntgeninterferenzen und Atomgröße. Physik. Z. **31**, 419—428 (1930)

Dennert, G., Höglund, S.: Pyruvate dehydrogenase of *Escherichia coli* K 12. Europ. J. Biochem. **12**, 502—507 (1970)

Durchschlag, H.: Röntgenkleinwinkeluntersuchungen am *E.-coli*-Pyruvat-Dehydrogenase-Core-Komplex. Abstr. Wintertagg. Ges. Biol. Chem. Konstanz 1973. Hoppe-Seylers Z. physiol. Chem. **354**, 205—206 (1973)

Durchschlag, H.: X-ray small-angle studies of the pyruvate dehydrogenase core complex from *Escherichia coli* K-12. Abstr. 3rd Int. Conf. on X-ray and neutron small-angle scattering, Grenoble 1973. J. appl. Cryst. **7**, 167 (1974)

Durchschlag, H.: X-ray small-angle studies of the pyruvate dehydrogenase core complex from *Escherichia coli* K-12. I. Overall structure of the core complex. Biophys. Struct. Mechanism, **1**, 153—168 (1975)

Durchschlag, H., Puchwein, G., Kratky, O., Schuster, I., Kirschner, K.: X-ray small-angle scattering of yeast glyceraldehyde-3-phosphate dehydrogenase as a function of saturation with nicotinamide-adenine-dinucleotide. Europ. J. Biochem. **19**, 9—22 (1971)

Eley, M. H., Namihira, G., Hamilton, L., Munk, P., Reed, L. J.: α-Keto acid dehydrogenase complexes. XVIII. Subunit composition of the *Escherichia coli* pyruvate dehydrogenase complex. Arch. Biochem. Biophys. **152**, 655—669 (1972)

Fernández-Morán, H., Reed, L. J., Koike, M., Willms, C. R.: Electron microscopic and biochemical studies of pyruvate dehydrogenase complex of *Escherichia coli*. Science **145**, 930—932 (1964)

Fischbach, F. A., Harrison, P. M., Anderegg, J. W.: An X-ray scattering study of the bacterial virus R17. J. molec. Biol. **13**, 638—645 (1965)

Glatter, O.: X-ray small angle scattering of molecules composed of subunits. Acta Phys. Austriaca **36**, 307—315 (1972)

Harrison, S. C.: Structure of tomato bushy stunt virus. I. The spherically averaged electron density. J. molec. Biol. **42**, 457—483 (1969)

Henning, U., Vogel, O., Busch, W., Flatgaard, J. E.: The pyruvate dehydrogenase complex of *E. coli* K-12. Structure and synthesis. In: Protein-protein interactions, 23rd Mosbach Colloquium (eds. R. Jaenicke, E. Helmreich), pp. 343—364. Berlin-Heidelberg-New York: Springer 1972

Hosemann, R.: Personal communication (1974)

Kahovec, L., Porod, G., Ruck, H.: Röntgenkleinwinkeluntersuchungen an dichtgepackten kolloiden Systemen. Kolloid-Z. **133**, 16—26 (1953)

Kirste, R., Porod, G.: Röntgenkleinwinkelstreuung an kolloiden Systemen. Asymptotisches Verhalten der Streukurven. Kolloid-Z. **184**, 1—7 (1962)

Koike, M., Reed, L. J., Carroll, W. R.: α-Keto acid dehydrogenation complexes. IV. Resolution and reconstitution of the *Escherichia coli* pyruvate dehydrogenation complex. J. biol. Chem. **238**, 30—39 (1963)

Kratky, O.: Die Abhängigkeit der Röntgen-Kleinwinkelstreuung von Größe und Form der kolloiden Teilchen in verdünnten Systemen. Monatsh. Chem. **76**, 325—349 (1947)

Kratky, O., Porod, G.: Die Abhängigkeit der Röntgen-Kleinwinkelstreuung von Form und Größe der kolloiden Teilchen in verdünnten Systemen, III. Acta Phys. Austriaca **2**, 133—147 (1948)

Mittelbach, P., Porod, G.: Zur Röntgenkleinwinkelstreuung kolloider Systeme. Die mittleren Durchschußlängen und die Kohärenzlänge eines kolloiden Systems; Kennzahlen zur Ermittlung von Teilchenform und Polydispersitätsgrad. Kolloid-Z. **202**, 40—49 (1965)

Perham, R. N., Thomas, J. O.: The subunit molecular weights of the α-keto acid dehydrogenase multienzyme complexes from *E. coli*. FEBS-Lett. **15**, 8—12 (1971)

Pilz, I., Glatter, O., Kratky, O.: Röntgenkleinwinkelstudien über die Substruktur von *Helix pomatia* Hämocyanin. Z. Naturforsch. **27b**, 518—524 (1972)

Porod, G.: Die Abhängigkeit der Röntgen-Kleinwinkelstreuung von Form und Größe der kolloiden Teilchen in verdünnten Systemen, IV. Acta Phys. Austriaca **2**, 255—292 (1948)

Porod, G.: Theorie der diffusen Röntgenkleinwinkelstreuung an kolloiden Systemen. Z. Naturforsch. **4a**, 401—414 (1949)

Porod, G.: Die Röntgenkleinwinkelstreuung von dichtgepackten kolloiden Systemen, I. Teil. Kolloid-Z. **124**, 83—114 (1951); Die Röntgenkleinwinkelstreuung von dichtgepackten kolloiden Systemen, II. Teil. Kolloid-Z. **125**, 51—57 and 108—122 (1952)

Porod, G.: Determination of general parameters by small-angle X-ray scattering. In: Small-angle X-ray scattering. Proc. Conf. at Syracuse University 1965 (ed. H. Brumberger), pp. 1—15. New York, London, Paris: Gordon and Breach 1967

Reed, L. J., Oliver, R. M.: The multienzyme α-keto acid dehydrogenase complexes. Brookhaven Symp. Biol. **21**, 397—412 (1968)

Schwartz, E. R., Reed, L. J.: α-Keto acid dehydrogenase complexes. XII. Effects of acetylation on the activity and structure of the dihydrolipoyl transacetylase of *Escherichia coli*. J. biol. Chem. **244**, 6074—6079 (1969)

Vogel, O., Beikirch, H., Müller, H., Henning, U.: The subunit structure of the *Escherichia coli* K-12 pyruvate dehydrogenase complex. The dihydrolipoamide transacetylase component. Europ. J. Biochem. **20**, 169—178 (1971)

Vogel, O., Henning, U.: Pyruvate dehydrogenase component subunit structure of the *Escherichia coli* K 12 pyruvate dehydrogenase complex. Europ. J. Biochem. **18**, 103—115 (1971)

Vogel, O., Henning, U.: The subunit structure of the *Escherichia coli* K 12 pyruvate-dehydrogenase complex. Dihydrolipoamide-dehydrogenase component. Europ. J. Biochem. **35**, 307—310 (1973)

Vogel, O., Hoehn, B., Henning, U.: The subunit structure of the pyruvate-dehydrogenase complex from *Escherichia coli* K-12. The core complex. Europ. J. Biochem. **30**, 354—360 (1972a)

Vogel, O., Hoehn, B., Henning, U.: Molecular structure of the pyruvate dehydrogenase complex from *Escherichia coli* K-12. Proc. nat. Acad. Sci. (Wash.) **69**, 1615—1619 (1972b)

Willms, C. R., Oliver, R. M., Henney, H. R., Mukherjee, B. B., Reed, L. J.: α-Keto acid dehydrogenase complexes. VI. Dissociation and reconstitution of the dihydrolipoyl transacetylase of *Escherichia coli*. J. biol. Chem. **242**, 889—897 (1967)

Zipper, P., Kratky, O., Herrmann, R., Hohn, Th.: An X-ray small angle study of the bacteriophages *fr* and R17. Europ. J. Biochem. **18**, 1—9 (1971)

Zipper, P., Schubert, D., Vogt, J.: Small-angle X-ray scattering studies on virus-like protein particles derived from bacteriophage *fr*. Europ. J. Biochem. **36**, 301—310 (1973)

Dr. Helmut Durchschlag
Biochemie II, Fachbereich Biologie
Universität Regensburg
D-84 Regensburg
Federal Republic of Germany